INVESTIGATION OF PROTEIN-INDUCED FORMATION OF LIPID DOMAINS AND THEIR DYNAMICS USING FLUORESCENCE ENERGY TRANSFER

Jenny R. Wright

A Thesis Submitted to the
University of North Carolina Wilmington in Partial Fulfillment
Of the Requirements for the Degree of
Master of Science

Department of Chemistry and Biochemistry

University of North Carolina Wilmington

2005

Approved by

Advisory Committee

Charles R. Ward

James H. Reeves

Paulo F. Almeida
Chair

Accepted by

_____
Dean, Graduate School

This thesis has been prepared in the style and format

consistent with the journal

Biochemistry

TABLE OF CONTENTS

ABSTRACT

An important feature in the current understanding of membrane structure is the existence of lipid domains. Lipid domain formation was observed in an experimental lipid bilayer system containing an equilibrium mixture of glycerophospholipids and raft lipids. Protein-lipid interactions in the equilibrium mixtures were observed when a peripheral membrane peptide was added. These interactions were measured using fluorescence energy transfer. Domain formation as a function of time was also investigated after the protein was added to the equilibrium mixture using stopped-flow fluorescence. Domain formation in vesicles containing 40% anionic lipid occurred in less than 1 s.

Domain dissipation was observed with stopped flow fluorescence spectroscopy in glycerophospholipid vesicles as well as in a mixture of glycerophospholipids and raft lipids by removing the peptide. Domain dissipation in vesicles containing glycerophospholipids with 20% anionic lipid occurred in approximately 5 s. Domain dissipation in vesicles containing rafts and 40% anionic lipid occurred in approximately 900 s and domain dissipation in vesicles containing rafts and 10% anionic lipid occurred in approximately 160 s. These timescales were compared to the off-rate of the peptide from the vesicles.

ACKNOWLEDGEMENTS

I would like to thank Dr. Paulo Almeida and Dr. Antje Almeida for their guidance and assistance. Thanks to my committee members, Dr. Jimmy Reeves and Dr. Dick Ward for their guidance. Also, thanks to all the chemistry faculty who helped me get where I am now.

Special thanks go to my parents, sister, and grandparents for their love and support. Also, special thanks to Allen Butler.

Thanks to Dr. Barbara Heath, for motivating me to get my masters in the first place. Thanks to Diana Wu for assistance, friendship, and introducing me to the lab.

Finally, I would like to thank Katy Magolan for her great friendship and her assistance with absolutely everything.

This work was supported in part by National Institutes of Health Grants GM59205 (University of Virginia, Charlottesville, VA) and GM072507 (University of North Carolina Wilmington).

LIST OF TABLES

Table Page

LIST OF FIGURES

Figure Page

INTRODUCTION

An important aspect of the current understanding of membrane structure is the existence of lipid domains. If proteins show preferential lipid interactions, these lipid domains can be induced through the binding of a protein to the membrane. The binding of peripheral proteins to membranes is crucial for biological processes such as signal transduction and vesicle trafficking (*1*). It has been suggested that the function of lipid diversity in the cell membrane is to regulate the formation of protein signal transduction complexes (*2*). It may also be that the role of lipids within the membrane is signal amplification through interactions between nearest neighbors (*3*).

Previous studies investigating the influence of lipid chemical structure on protein binding using a fluid, binary lipid system indicated that lipid and protein clustering are correlated (*3*). Small, cooperative interactions between lipids can be coupled to protein binding, leading to domain formation. If these interactions are concentrated in the same domain, these events will be enhanced in magnitude and specificity. Lipid and protein interactions cause reorganization of the membrane, and can lead to large changes in domain formation when a protein binds preferentially to one of the lipids.

Hinderliter et al (*2*) investigated the effect of altering lipid chemical structures on the net interaction free energy and how it influenced lipid and protein domain formation. This was done to explore the reason for lipid diversity in eukaryotic membranes, especially slight variations in the acyl chains. They suggested that the role of lipid diversity is to provide an on-off switch for a signaling event at the membrane level.

The membranes of eukaryotic cells contain three main classes of lipids: glycerophospholipids, sphingolipids, and cholesterol (*4*). Glycerophospholipids, also called phosphoacylglycerols, are phosphate esters of the three-carbon alcohol, glycerol. The fatty acyl chains usually have an even number of carbon atoms, with 16- and 18-carbon acids being the

most common. The chains may also contain *cis* unsaturation (Fig. 1A, B). Sphingolipids (Fig. 1C), a second group of polar lipids, have the parent structure of the amino alcohol sphingosine. Finally, cholesterol is an isoprenoid compound with four fused rings, a short aliphatic chain, and a single hydroxyl group (Fig 1D).

Domains rich in cholesterol and the sphingolipid sphingomyelin, called 'rafts', have recently received a significant amount of attention (*4-9*). It is thought that these large protein-lipid complexes could be important in signal transduction at the level of the cell membrane by functioning as platforms for the attachment of proteins (*10*). The involvement of rafts has been implied in several kinds of physiological and pathological processes (*10*).

Cell membranes are two-dimensional liquids, and hydrated bilayers undergo phase transitions as a function of temperature. The main transition has been described as an ordered-to-disordered phase transition. The two phases are labeled solid ordered (s_o), below the transition temperature, and liquid disordered (l_d), above that temperature (*11*). Cholesterol and phospholipids can form a liquid-ordered (l_o) phase that could coexist with a cholesterol-poor, liquid-disordered (l_d) phase, which permits phase coexistence in wholly liquid phase membranes (*12, 13*).

The dynamics of domain formation and dissipation have received little attention. Collado et al. (*14*) investigated domain formation in sphingomyelin/cholesterol membranes using spin-label electron spin resonance spectroscopy. They found that the rate at which the lipids exchange between the two fluid phases, liquid ordered and liquid disordered, must be considerably slower than the translational diffusion rates in the liquid disordered phase (*14*). Thus, it is possible that domain dissipation would be a slower process than diffusion, and its kinetics could be measured by stopped-flow fluorescence.

A

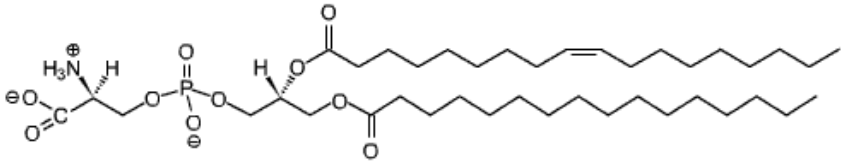

B

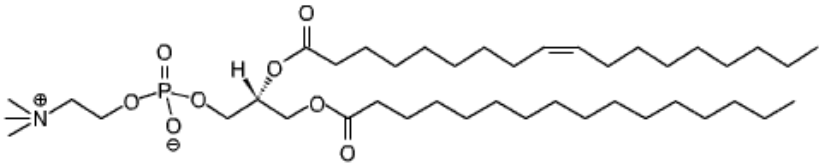

C

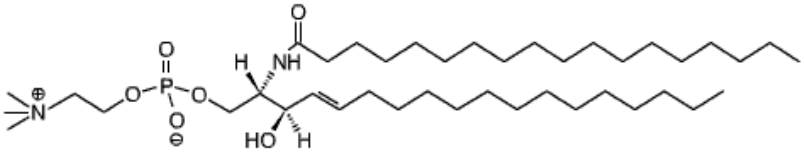

D

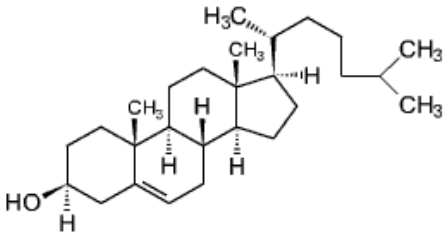

FIGURE 1. Examples of structures of common lipids found in the cell membrane: glycerophospholipids POPS **(A)** and POPC **(B)**, sphingolipids **(C)**, and cholesterol **(D)**. Structures are from avantilipids.com.

The peripheral membrane protein, myristoylated alanine-rich C kinase substrate (MARCKS), is the major protein kinase C (PKC) substrate in many cell types (*15*). The basic effector region of MARCKS (residues 151-175) comprises the binding site for membranes, and has the amino acid sequence KKKKKRFSFKKSFKLSGFSFKKNKK. The peptide carries 13 positive charges, one for each lysine, which is electrostatically attracted to anionic lipids.

Domains were observed using fluorescence resonance energy transfer (FRET). FRET is a distance-dependent interaction between the excited states of fluorescent molecules in which excitation is transferred from a donor molecule to an acceptor molecule without emission of a photon (*16*). Because this technique is useful for measuring changes in molecular proximity, changes in domain sizes can be measured.

Experimentally, domain formation was observed in vesicles containing sphingomyelin, cholesterol, and a glycerophospholipid such as 1-palmitoyl-2-oleoyl-s*n*-glycero-3-phosphoserine (POPS) or 1-palmitoyl-2-oleoyl-s*n*-glycero-3-phosphocholine (POPC) (see Fig. 1). These vesicle mixtures consist of a l_o phase containing sphingomyelin and cholesterol coexisting with the POPS or POPC l_d phase, causing a phase separation within the vesicles. The two fluorophores were attached to lipids containing the same acyl chains as POPS and POPC. This ensured that the probes would mimic the behavior of the glycerophospholipids. Because the fluorophores and the glycerophospholipids contained the same chains, the probes are assumed to partition into the same domains as POPS and POPC due to the phase separation existing in the vesicle mixtures.

Domain formation was induced or enhanced using the effector region of MARCKS peptide. The timescales for domain formation and dissipation were not known. Domain formation and dissipation were observed using stopped-flow fluorescence when MARCKS was

added to or removed from the membrane. Other vesicles containing mixtures of different lipids were also observed to illustrate domain formation and their time scales in systems different from those containing sphingomyelin/cholesterol.

MATERIALS AND METHODS

Materials

1-Palmitoyl-2-oleoyl-*sn*-glycero-3-phosphocholine (POPC), 1-palmitoyl-2-oleoyl-*sn*-glycero-3-phosphoserine (POPS), 1-palmitoyl-2-oleoyl-*sn*-glycero-3-phosphoethanolamine (POPE), 1,2-dimyristoleoyl-*sn*-glycero-3-phosphocholine (di-14:1PC), and brain (porcine) sphingomyelin (SM) were purchased from Avanti Polar Lipids, Inc. (Birmingham, AL). Cholesterol (Cho) was from ICN Biomedicals Inc. (Aurora, Ohio). Myristoylated alanine-rich C kinase substrate (MARCKS) (151-175) was a gift from Dr. Rodney Biltonen (University of Virginia). 4-Chloro-7-nitrobenz-2-oxa-1,3-diazole chloride (NBD chloride) and Marina Blue® succinimidyl ester (MB succinimidyl ester) were from Molecular Probes (Eugene, OR); NBD-MARCKS was from Sigma-Genosys. Molecular sieves (4A, beads, 4-8 mesh), sodium molybdate dihydrate, and hydrazine sulfate were purchased from Aldrich Chemical Company (Milwaukee, WI). Dimethylformamide (DMF), potassium chloride (KCl), and potassium carbonate (K_2CO_3) were purchased from Mallinckrodt Baker, Inc. (Paris, KY). Sulfuric acid and perchloric acid were from EM Science (Darmstadt, Germany). Dichloromethane (CH_2Cl_2), chloroform ($CHCl_3$), and methanol (MeOH) were purchased from Allied Signal Burdick & Jackson (Muskegon, MI). 3-(N-Morpholino)propane-sulfonic acid (MOPS) was from MERCK (Darmstadt, Germany). Azide and [Ethylenebis(oxy-ethylenenitrilo)] tetra-acetic acid (EGTA) were from Acros (NJ). Potassium hydroxide (KOH) was from Fisher Scientific (Fairlawn, NJ). Thin layer chromatography (TLC) plates were purchased from Whatman Internation Ltd. (Maildstone, England); and Uniplate® preparatory plates were purchased from Analtech, Inc. (Newark, DE).

Buffer

Concentrated stock (10X) buffer contained 0.20 M MOPS, 1.0 M KCl, 0.2% azide, and 1.0 mM EGTA, and was refrigerated. Buffer used for experiments was diluted from the stock buffer 1:10. The pH was adjusted to 7.50 using KOH.

Synthesis of Fluorescent Lipid Probes

MB and NBD were chosen because of their large energy transfer capacity. The probes were attached to a lipid moiety so that they would mimic the behaviors of the lipids. POPE was chosen because it has a free amino group and has the same acyl chains as POPS and POPC, therefore partitioning into those lipid domains.

Synthesis of MB-POPE

Molecular sieves were dried for five hours at 80ºC. $CHCl_3$ and DMF were then poured over the molecular sieves and allowed to dry overnight. K_2CO_3 was dried in a dessicator under vacuum for about 5 hours. Stock POPE solution in $CHCl_3$ was evaporated in a rotoevaporator (Büch 3000 rotovap) to remove solvent and was then re-dissolved in dry $CHCl_3$. Starting with 5 mg of MB, the mass of POPE to be reacted was determined such that it was 1.1:1 (POPE:MB mole ratio). MB was dissolved in as little DMF as possible (approximately 0.3 mL of DMF). $K_2CO_{3(s)}$, 1:1 ratio with POPE, was dissolved in 0.2 mL of DMF, and POPE was then added to this solution. The MB/DMF solution was then added drop wise to the POPE/ $K_2CO_{3(s)}$/DMF solution. The mixture was stirred in the dark overnight.

The mixture was analyzed by TLC, with CH_2Cl_2:MeOH 2:1 (v/v) as the solvent, on a TLC plate. The MB was identified with UV light, and the POPE was identified using the

Zinzade reagent (*17*). The Zinzade reagent, which exposed the phosphorus head group of the probe, was prepared by dissolving sodium molybdate dihydrate (6.85 g) and hydrazine sulfate (0.4 g) in 100 mL of distilled water. A volume of 250 mL of concentrated sulfuric acid was added, and the mixture was allowed to cool. 600 mL of distilled water was then added.

Separation was carried out on a Uniplate® (20 x 20 cm, 1000 microns) using the solvent system CH_2Cl_2:MeOH (3.5:1). The pure product band was left on the origin. The band corresponding to MB-POPE was scraped off with a razor blade and the fluorescent lipid was recovered and then separated from the silica with a sintered glass funnel using CH_2Cl_2:MeOH (2:1), (a 10 mL mini column plugged with glass wool could also be used for the separation). CH_2Cl_2 was added to the mixture before evaporating on the rotavap to help remove all the MeOH. After evaporating all solvent, dry $CHCl_3$ was added to re-dissolve the product. The concentration of the product was determined using the phosphorous assay (*18*). Using this concentration, the molar absorptivity of MB in MeOH and in CH_2Cl_2 was determined using a CARY 1E UV-Visible Spectrophotometer. The molar absorptivity of MB was estimated to be 15,674 at 368 nm in MeOH, and 8,535 at 341 nm in CH_2Cl_2. The percent yield of this reaction was 35%. The product structure can be seen in Fig. 2.

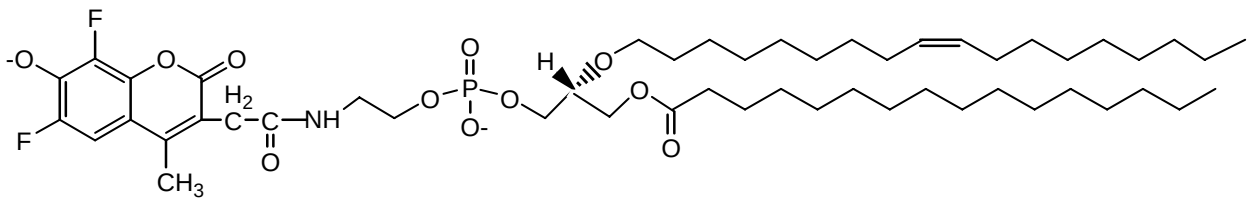

FIGURE 2. Structure of MB-POPE at pH 7.5.

Synthesis of NBD-POPE

Molecular sieves were dried for five hours at 80ºC. $CHCl_3$, and MeOH, were then poured over the molecular sieves and allowed to dry about 5 hours. K_2CO_3 was dried in a vacuum dessicator for about 5 hours. Stock POPE solution in $CHCl_3$ was evaporated in a rotoevaporator to remove solvent and was then re-dissolved in dry $CHCl_3$. Starting with 5 mg of NBD-Cl, the reacting volume of POPE was determined such it was 1.5:1 (POPE:NBD mole ratio). NBD was dissolved in $CHCl_3$:MeOH (50:50 (v/v)), (as little as possible, approximately 0.3 mL). $K_2CO_{3(s)}$, 1.1:1 mole ratio with POPE, was added to POPE, and then the NBD solution was added drop wise to the POPE/ $K_2CO_{3(s)}$ solution. The mixture was stirred in the dark for approximately 30 minutes.

The reaction course was analyzed by TLC using the solvent CH_2Cl_2:MeOH:H_2O 65:25:4 (v/v), on a TLC plate. The NBD was identified with UV light, and the POPE was identified using the Zinzade reagent. TLC showed no fluorescent product after 30 minutes. Therefore, the mixture was allowed to react overnight. Only a small amount of product was seen, so 2.5 mg NBD (half of original amount) was added to drive the reaction toward the product. It was allowed to react for about more 5 hours.

Separation was carried out on a Uniplate® (20 x 20 cm, 1000 microns) using solvent system CH_2Cl_2:MeOH (4:1), and then separated in a sintered glass funnel using CH_2Cl_2:MeOH (4:1) followed by CH_2Cl_2:MeOH (3:1). After evaporating all solvent with the rotavap, dry $CHCl_3$ was added to re-dissolve the product. The concentration of the product was determined using a CARY 1E UV-Visible Spectrophotometer. NBD has a molar absorptivity of 21,000 at 463 nm in MeOH (*19*). The reaction had 18% yield.

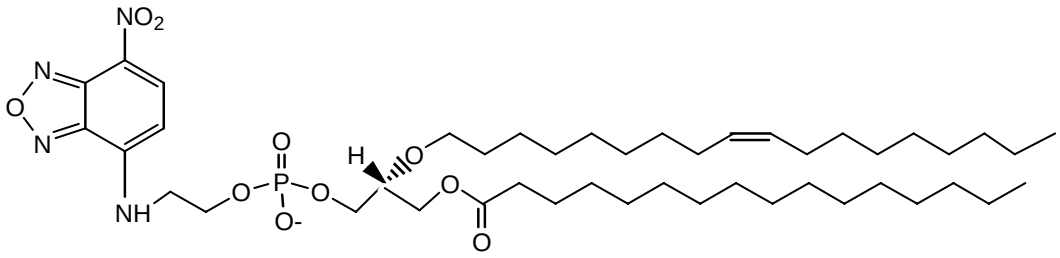

FIGURE 3. Structure of NBD-POPE at pH 7.5

Preparation of Large Unilamellar Vesicles (LUV)

Mixtures of lipids were prepared by aliquotting stock solutions of lipid into a round bottom flask. The chloroform solvent was evaporated from the mixture using a rotoevaporator and the lipid film thus obtained was then allowed to dry under vacuum for approximately 4 hours. All vesicle mixtures containing fluorescent probes were kept in the dark. Lipids were hydrated using MOPS buffer (pH 7.50) and vortexed for a few minutes. A suspension of multilamellar vesicles (MLV) was thus formed. Hydration was performed above the gel-fluid phase transition temperature of the highest melting lipid: at room temperature for PS and PC vesicles and at 70°C for vesicles containing SM and Cho. LUV were prepared by extruding 2 mL of the MLV dispersion 10 times through two stacked Nucleopore polycarbonate filters with pore size 0.1 μm and Whatman Nucleopore drain disk of 2.5 mm pore size, using a water-jacketed, high-pressure extruder from Lipex Biomembranes Inc. The dispersion was maintained above the phase transition temperature throughout the extrusion process: at room temperature for PS and PC vesicles and at 70°C for SM and Cho vesicles. All hydrated lipid samples were stored in the dark under a nitrogen atmosphere at room temperature. The concentration of the vesicles was verified using a modified version of the Bartlett phosphate assay (*19*).

Peptide Preparation

Solutions of the MARCKS peptide were prepared by weighing the lyophilized peptide and hydrated with distilled water. The concentration was confirmed by averaging results from gravimetric measurements, the Bradford assay (*20*), and Fluorescamine assay (*21*). The ratios of the concentrations estimated by each method were 1.00/0.652/0.480 for gravimetric measurements, Bradford assay and Fluorescamine assay, respectively.

Fluorescence Spectroscopy Measurements

Fluorescence measurements were recorded on a SLM Aminco 8100 Spectrofluorometer. The changes in domain size were monitored using fluorescence resonance energy transfer (FRET) from a donor to an acceptor molecule. N-(6,8-difluoro-7-hydroxy-4-methyl-2-oxo-2H-1-benzopyran-3-yl)acetyl) 1-palmitoyl-2-oleoyl-*sn*-glycero-3-phosphoethanolamine, Marina Blue®-POPE (MB-POPE) and N-((7-nitrobenz-2-oxa-1,3-diazole)-1-palmitoyl-2-oleoyl-*sn*-glycero-3-phosphoethanolamine (NBD-POPE) were selected as the energy transfer pair, where MB is the donor and NBD is the acceptor.

Steady State Fluorescence

For steady state measurements, the excitation wavelength for MB was 367 nm, and emission spectra were recorded from 400 nm to 600 nm, encompassing both the MB and NBD emission peaks. Excitation and emission monochromator band-passes were 2 nm and 8 nm, respectively. A 10 mm path-length quartz cell (Genuine McCarthy Precision Cell, No.2 type 9F) was used for measurements. Vesicles were used at a concentration of 100 μM.

Stopped-Flow Fluorescence

The timescales for domain dynamics were obtained using the SLM-Aminco 8100 adapted with a RX2000 rapid kinetics spectrometer accessory (Applied Photophysics).
The excitation wavelength was 367 nm (MB excitation), and emission was measured as a function of time at 535 nm (NBD emission). In domain formation experiments, excitation and emission monochromator band-passes were 4 nm and 16 nm, respectively. In dissipation experiments, excitation and emission monochromator band-passes were 1 and 16 nm,

respectively. Before placing the sample in the stopped-flow, the stopped-flow was flushed with detergent Triton-X100. It was then rinsed with approximately 50 mL of buffer before vesicle mixtures were placed in the stopped-flow for measurements.

Since the vesicles were mixed using the two syringes, they were placed in the syringe at a concentration of 200 μM, so that, when they were mixed and diluted by a factor of two, the concentration would then be 100 μM, which was the concentration used in the steady-state measurements. Each measurement was repeated between five and ten times so that the results could be averaged to reduce the noise in the spectra.

Domain formation experiments were performed by mixing the vesicles with MARCKS in the stopped-flow apparatus. The emission was compared to a baseline. Fluorescence would increase with the addition of peptide if it is promoting domain formation because this should occur concomitantly with an increase in energy transfer.

Domain dissipation was observed using similar conditions as the domain formation experiments. In the dissipation experiments, the vesicles were pre-incubated with the MARCKS so that the domains would be present initially, corresponding to a high level of FRET. These vesicles were then mixed with acceptor vesicles, which contained the same lipids but no probes, and were at a concentration ten times greater than the incubated lipids. The acceptor vesicles were therefore presumed to extract the MARCKS from the donor vesicles, which would cause the domains to dissipate and energy transfer to decrease. To ensure that the timescale that was measured readily corresponded to domain dissipation, and not just to MARCKS dissociation from the membrane, the dissipation timescales were compared to the timescales of MARCKS desorption from the membrane.

The timescales for MARCKS desorption were determined using vesicles containing only MB and MARCKS labeled with NBD (NBD-MARCKS). In these experiments, NBD-MARCKS was pre-incubated with vesicles containing MB, allowing for energy transfer to occur between the NBD on the MARCKS when it binds domains on the membrane containing MB-POPE. When this suspension is mixed with acceptor vesicles that contain lipids with no probe in ten-fold excess, the acceptors will extract the NBD-MARCKS, and the energy transfer will decrease. The timescale for this event directly indicates how long it takes for the MARCKS to come off the membrane.

RESULTS AND DISCUSSION

Monitoring Lipid Domain Formation in Steady State Fluorescence

Lipid domain formation was observed using fluorescence resonance energy transfer. Transfer of energy from an excited state fluorophore to an acceptor can occur if there is spectral overlap between the fluorescence emission spectrum of the donor and the absorption spectrum of the acceptor (*16*). MB is the donor and NBD is the acceptor. This provides a nice pair because the emission spectrum of MB has significant overlap with the excitation spectrum of NBD (Fig. 4). The MB is excited at 367 nm where there is no absorption of NBD, and the emission of both MB and NBD are observed.

The overlap integral J(λ) expresses the degree of spectral overlap between the donor emission and acceptor excitation (22),

$$J(\lambda) = \int_0^\infty F_D(\lambda)\varepsilon_A(\lambda)\lambda^4 d\lambda ,$$

where $F_D(\lambda)$ is the corrected fluorescence intensity of the donor in the wavelength range $\lambda + \Delta\lambda$, with the total intensity (area under the curve) normalized to unity and $\varepsilon_A(\lambda)$ is the extinction coefficient of the acceptor at λ. The distance at which FRET is 50% efficient, called the Förster distance (R_0), is typically in the range of 20-60 Å (*22*). When the donor-to-acceptor distance is equal to R_0 then the transfer efficiency is 50%.

The overlap integral was calculated for the energy transfer pair by first plotting the spectral overlap and determining the area under that curve with the integral function using the commercially available Prostat program. It was determined to be 49 Å. This is a large value, which is indicative of a large amount of energy transfer that can occur with this pair. The efficiency of energy transfer is high for distances less than 49 Å. Thus, the

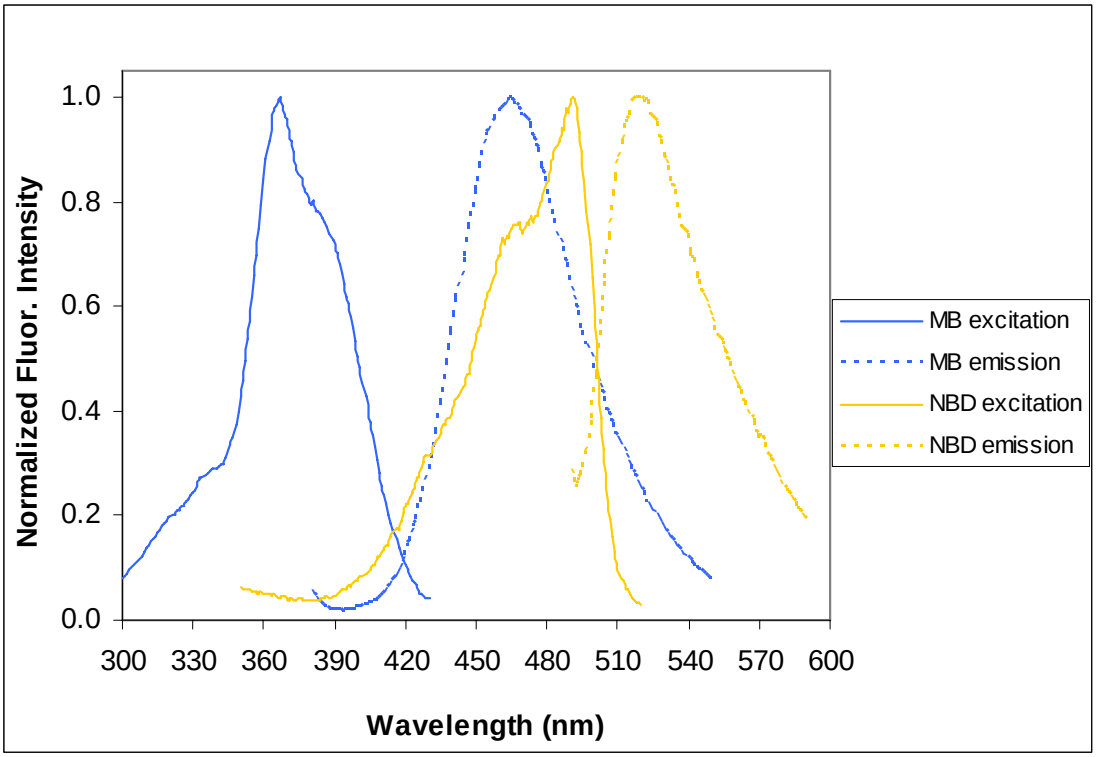

FIGURE 4. Excitation (solid) and emission (dotted) spectra of MB (blue) and NBD (orange) showing the overlap of the MB emission and NBD absorption.

probes do not need to be in contact to sense each other; they can transfer energy at a distance of about 6 lipids since the diameter of a lipid is about 8 Å. Energy transfer drops quickly for distances longer than 49 Å, with a R_0^6 dependence on distance between fluorophores (*22*).

Vesicles of SM:Cho:POPS

Domain formation was observed using steady state fluorescence in vesicles containing SM, Cho, POPS, and the fluorescent energy transfer pair MB-POPE and NBD-POPE. These vesicles contain two types of domains (or phases), one rich in POPS and the other rich in SM/Cho. MB was excited at 367 nm and the emission was scanned from 400 nm to 600 nm. The probe concentrations present in all vesicles were determined experimentally such that there would not be much energy transfer in the absence of peptide, but present a significant amount of energy transfer, representing the increase in domain formation, once a final peptide concentration had been reached. Various vesicle mixtures were prepared and fluorescence emission scans were recorded, where the percentages of both MB-POPE and NBD-POPE were varied. The percentage of probe that resulted in the highest sensitivity to peptide addition was determined to be 1 mole % MB and 1 mole % NBD. The fluorescence intensity was observed as a function of MARCKS concentration in 100 μM vesicles containing equimolar amounts of SM and Cho and 20, 40, 60, and 80 mole % POPS (Fig. 5). MARCKS peptide was then titrated onto the vesicles to obtain the maximum amount of energy transfer that could occur within these vesicles. As the peptide concentration increased, energy transfer increased until the peptide concentration reached about 2.5 μM, at which point the amount of energy transfer leveled off. This is interpreted to mean that the domain sizes had stopped increasing; the anionic lipid becomes saturated with peptide at this concentration. Thus, when the concentration is further increased to 5 μM, there is no more change in domain size.

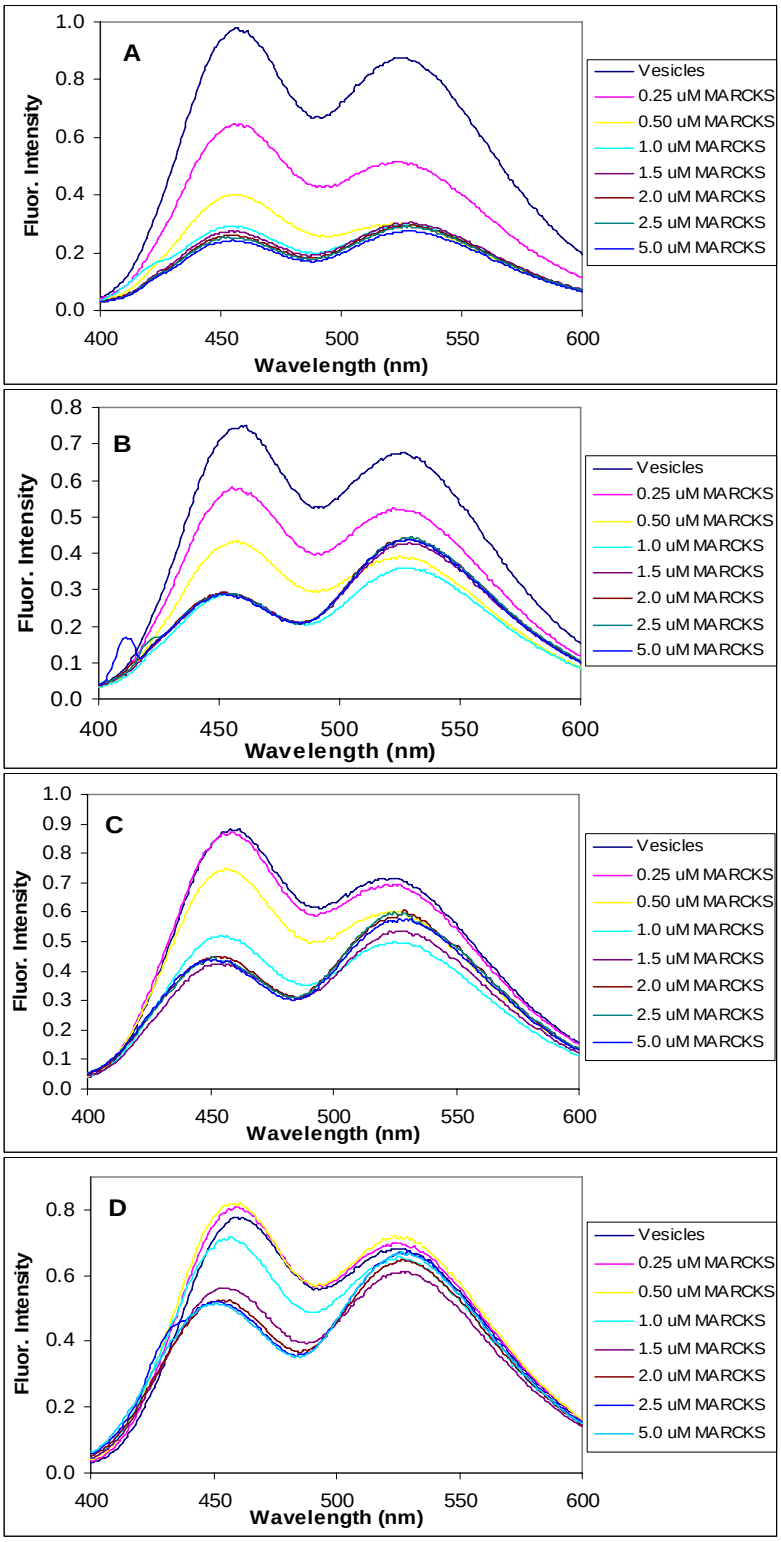

FIGURE 5. Comparison of the experimental fluorescence intensity as a function of MARCKS peptide concentration for various mole percent of 100 μM SM:Cho:POPS, MB-POPE and 1% NBD-POPE vesicles: **(A)** 40:40:18, **(B)** 30:30:38, **(C)** 20:20:58, **(D)** 10:10:78.

The relative amount of energy transfer was estimated by dividing the NBD emission peak (528 nm) by the MB emission peak (459 nm) for each of the SM/Cho/POPS vesicle systems (Fig. 6). The greatest increase in energy transfer was observed in vesicles containing 40% POPS. This is interpreted to mean that this system provides the greatest increase in domain formation. The 60% POPS and 80% POPS show an increase in energy transfer, but not as much as the 40% POPS. The 20% POPS has no increase in energy transfer; it shows an initial decrease before leveling off. This is possibly a result of having so much more MARCKS compared to the amount of POPS present that MARCKS competes for the POPS. MARCKS could be binding to the POPS or probes and separating them, which would cause a decrease in domain size.

With increasing MARCKS concentration, there is an initial decrease in the overall fluorescence intensity, which can be seen in Fig. 5. When MARCKS was added, the solution became visibly cloudy in the cuvette. The cause of this drop is thought to be the result of light scattering. When the MARCKS is added, it probably agglutinates vesicles or causes their morphology to change, leading to an increase in light scatter. To investigate this problem in more detail, the scatter at 90° was measured for 100 μM vesicles containing SM:Cho:POPS (40:40:19) 1% MB-POPE and SM:Cho:POPS (40:40:19) 1% NBD-POPE. The excitation and emission wavelength were set to 300 nm, and the drop in fluorescence intensity reflects an increase in light scatter (Fig. 7). This wavelength was chosen because neither probe absorbs at 300 nm, and because scattering varies as λ^4 (*22*), so a smaller wavelength is more sensitive to scatter.

As seen in Fig. 7, the fluorescence decreases in both the MB and NBD vesicles. This probably means there is no influence of MARCKS on the MB fluorescence signal itself.

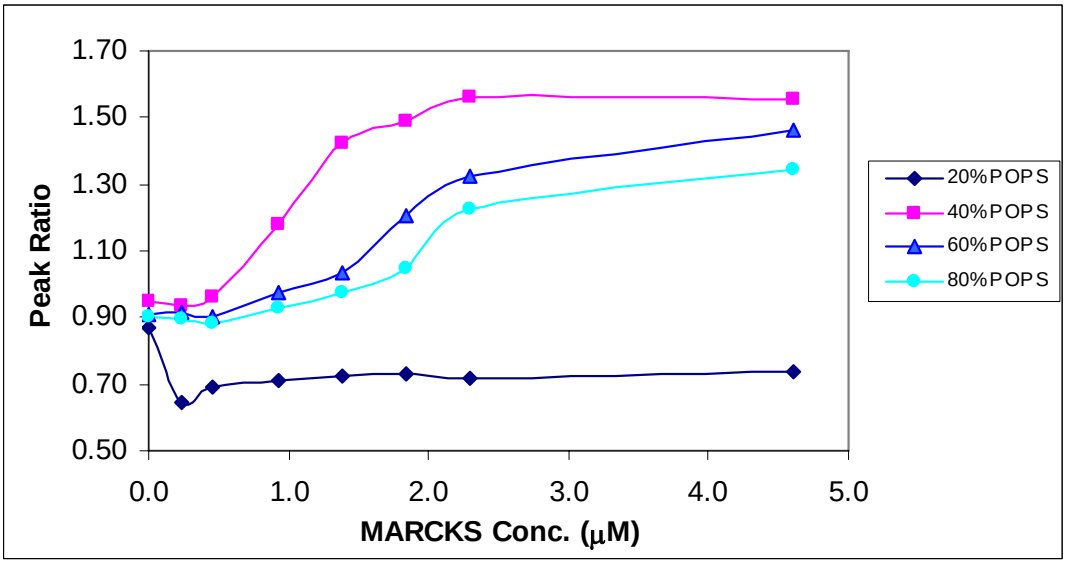

FIGURE 6. Energy transfer as a function of MARCKS concentration in 100 μM vesicles containing equal mole ratios of SM/Cho and 20% POPS, 40% POPS, 60% POPS, or 80% POPS.

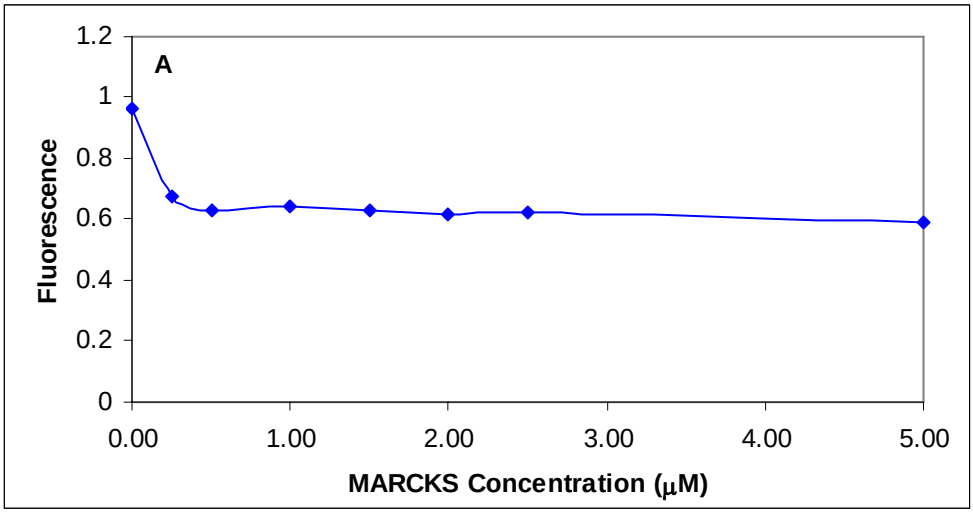

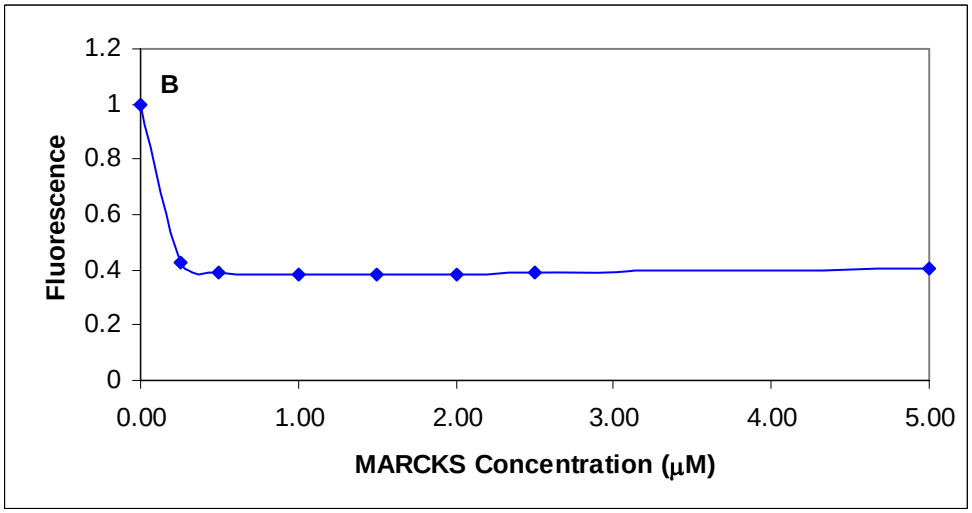

FIGURE 7. 90° light scatter at 300 nm for 100 μM vesicles containing SM:Cho:POPS (40:40:19) 1% MB-POPE **(A)** and SM:Cho:POPS (40:40:19) 1% NBD-POPE **(B)**.

Rather, the fluorescence intensity drop is probably caused by light scattering in both cases because it occurs in both types of vesicles. The light scatter levels off at 0.5 μM. In comparison, energy transfer increases until 2.5 μM (Fig. 6). This shows that the increase in energy transfer is not dependent on the increase in scatter.

Because the light scatter may be a result of vesicle agglutination, it was necessary to determine if the energy transfer that was measured was taking place within domains in the individual vesicles or between vesicles. 100 μM vesicles were prepared containing a mixture of vesicles consisting of one probe each: 50 μM SM:Cho:POPS (40:40:19) 1% MB, and 50 μM SM:Cho:POPS (40:40:19) 1% NBD (Fig. 8). The vesicles were in equimolar amounts in the cuvette for fluorescence measurements, so that half of the vesicles would contain one probe and half would contain the other probe to the same final vesicle concentration as in the previous experiments. When MARCKS was added, energy transfer would only occur if it were being transferred from one vesicle to another.

As seen in Fig. 8, the NBD emission peak at 535 nm is extremely small, almost nonexistent, which indicates that any energy transfer occurring between vesicles is negligible. This shows that energy transfer is taking place in domains containing POPS, and the contribution from inter-vesicle energy transfer is insignificant.

NBD-POPE was analyzed separately (Fig.9). The MB peak was observed in 100 μM vesicles that were excited at 367 nm, and the emission was scanned from 400 to 600 nm (Fig. 9A). The NBD peak was obtained using 100 μM vesicles that were excited at 490 nm and the emission was scanned from 500 to 600 nm (Fig. 9B).

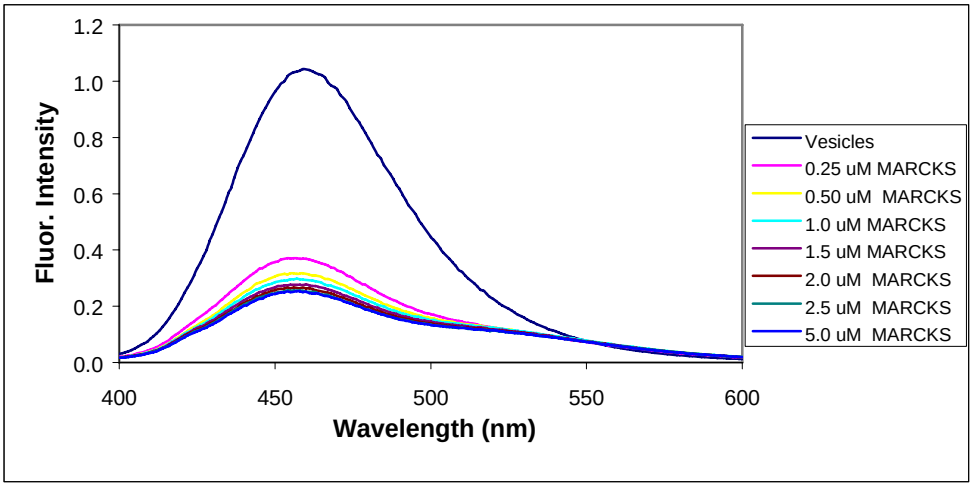

FIGURE 8. 100 μM SM:Cho:POPS (40:40:19) 1% MB-POPE and 100 μM SM:Cho:POPS (40:40:19) 1% NBD-POPE mixed 50:50 (v:v), as a function of MARCKS peptide.

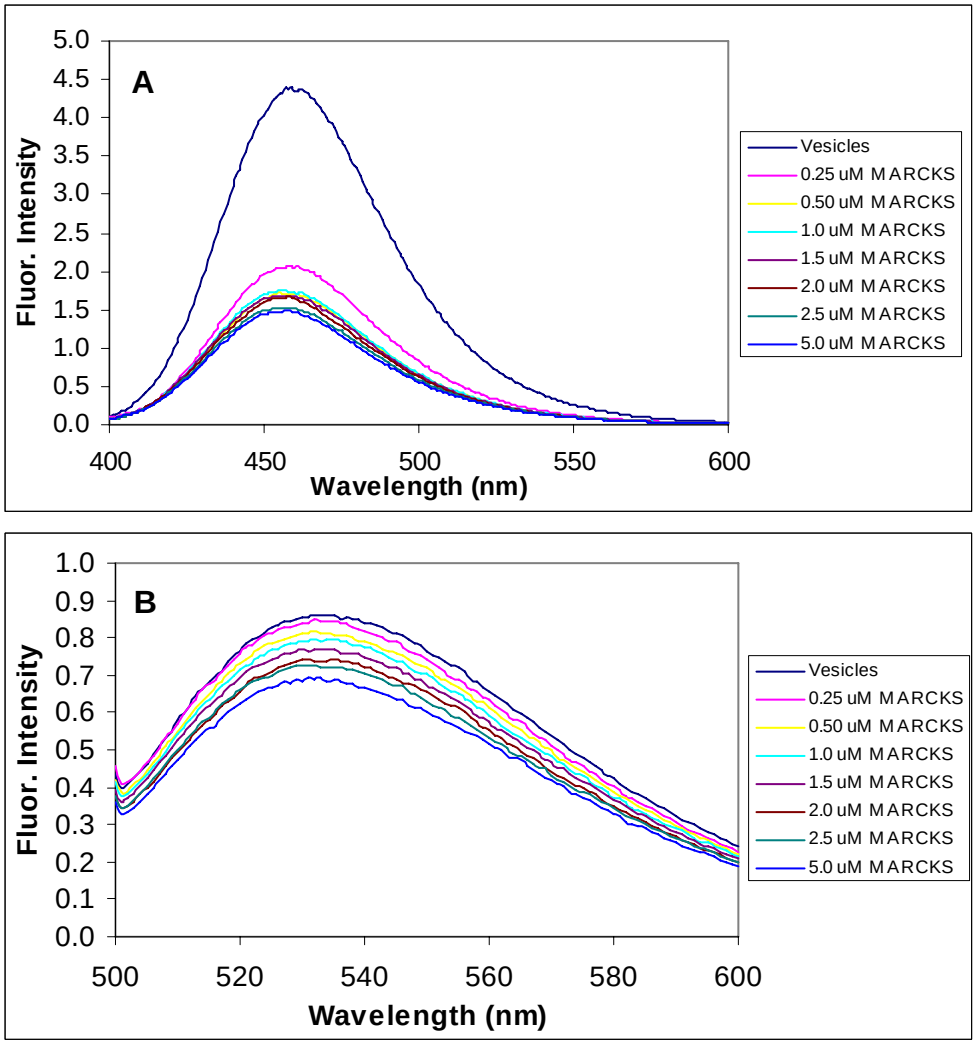

FIGURE 9. The emission spectra of SM:Cho:POPS (40:40:19) 1% MB-POPE **(A)**, and SM:Cho:POPS (40:40:19) 1% NBD-POPE **(B)**, as a function of MARCKS peptide.

As seen in Fig. 9, there is a drop in fluorescence intensity, but the drop is much less in the NBD peak than in the MB peak. Scattering is inversely proportional to λ^4 (*23*) therefore shorter wavelengths are scattered much more than longer wavelengths. This is more evident when the probes were analyzed separately because the excitation wavelength was 490 nm for NBD, but it was 367 nm for MB and the vesicles containing both probes (see Fig. 5). The decrease in fluorescence intensity seen in the NBD peak with the addition of MARCKS also illustrates that there is not some artifact resulting from a direct effect of MARCKS on the NBD peak that would cause the intensity increase in the emission scans seen in Fig. 5. This confirms that the increase in fluorescence intensity for the NBD peak seen in Fig. 5 is from energy transfer.

The efficiency of energy transfer was calculated using information from the plot with 20% POPS, 1%MB and 1%NBD in Fig. 5A, and the plot with 20% POPS and 1% MB in Fig. 9A. These two sets of spectra were obtained using the same spectrofluorometer settings and the efficiency of energy transfer was calculated at
459 nm (MB emission peak) using the formula (*22*),

$$Eff = 1 - \frac{E_{D/A}}{E_D}$$

where $E_{D/A}$ is the emission of the donor (MB) in the presence of the acceptor (NBD), and E_D is the emission of the donor (MB) in the absence of acceptor. Efficiency of energy transfer in 100 μM vesicles containing SM:Cho:POPS (40:40:20) as a function of MARCKS concentration can be seen in Fig. 10.

As seen in Fig. 10, there is a significant amount of energy transfer (78%) present before the addition of MARCKS. With the first addition of MARCKS, the efficiency drops, and then rises to about 84% at 1 μM MARCKS.

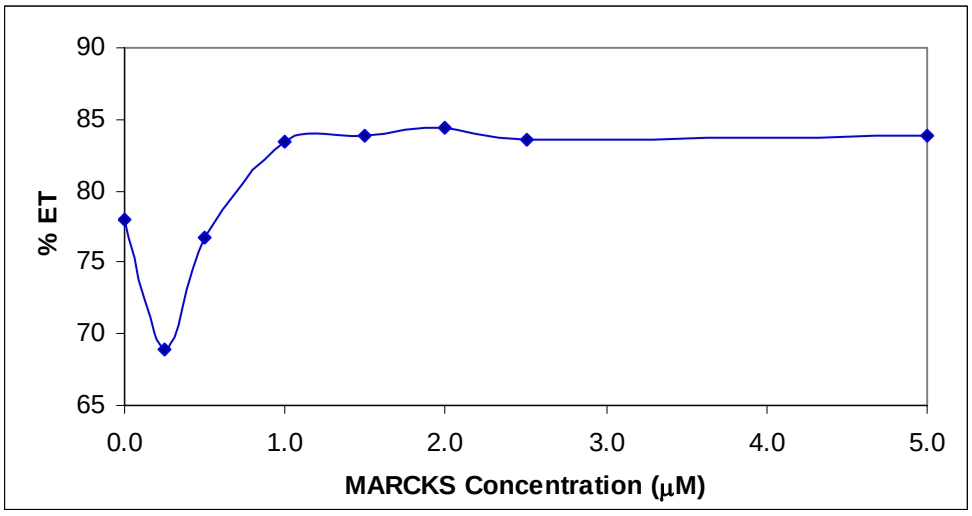

FIGURE 10. The percent of energy transfer in 100 μM vesicles containing SM:Cho:POPS (40:40:20) as a function of MARCKS concentration.

This experiment was repeated with vesicles containing 40% POPS and also with vesicles containing 20% POPS. A curve was constructed using the peak ratios calculated by dividing the NBD emission peak (528 nm) by the MB emission peak (459 nm) for both the 20% POPS and 40% POPS, as well as the efficiency of energy transfer for both 20% POPS and 40% POPS (Fig. 11).

A binding curve was fit to the data using a non-linear least squares analysis,

$$y = 100\left(\frac{k\left(x - x_0\right)}{1 + k\left(x - x_0\right)}\right),$$

where the values obtained from the fit were k = 10, and $x_0 = 0.5$. A binding curve was chosen for this data set because the data was expected to level off at 100% energy transfer. This curve, which has no physical significance, provides an easy way to estimate the efficiency of energy transfer without having to measure it using the MB peak in vesicles containing both probes, and the MB peak in vesicles containing only MB-POPE. This result indicates that the peak ratio is proportional to energy transfer and provides a simple, internal method of estimating energy transfer.

Vesicles of SM:Cho:POPC

Vesicles containing POPC were analyzed to compare with results from the POPS experiments. Similar to the POPS vesicles, these vesicles contain two types of domains, one rich in POPC, the other in SM/Cho. POPC was chosen because it carries no net charge as compared to the negatively charged POPS. It was hypothesized that the MARCKS would not bind well enough to the POPC to induce domain formation, so it was used to ensure that MARCKS was agglutinating POPS, and not only the probes.

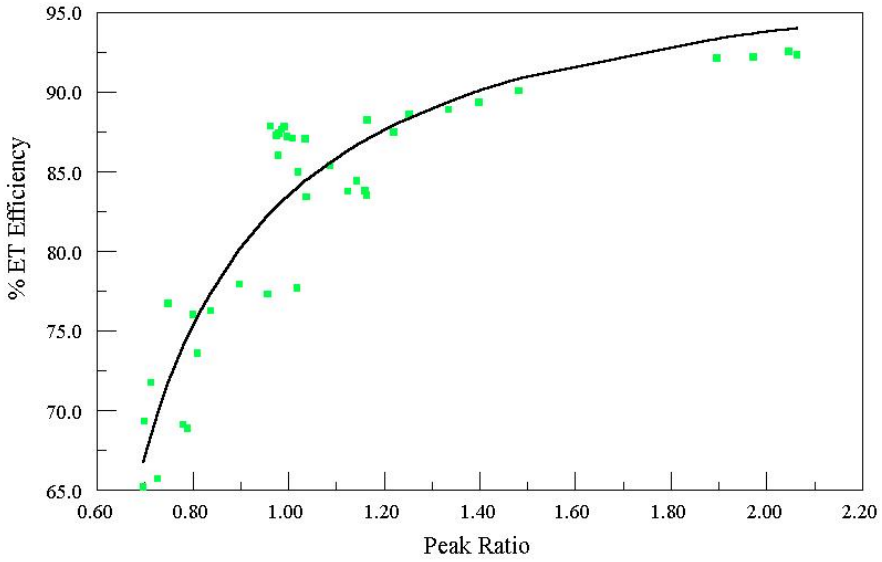

FIGURE 11. Efficiency of energy transfer versus peak ratio of vesicles containing 20% POPS and 40% POPS.

Steady state fluorescence was used to observe vesicles containing SM, Cho, POPC, and the fluorescent energy transfer pair MB-POPE and NBD-POPE. The same mole ratios were used as in the POPS experiments with POPS-containing vesicles, now using POPC instead of POPS as the unsaturated lipid in the vesicle system. The same probe concentrations were used in the POPC vesicles as in the POPS vesicles: 1 mole % MB-POPE and 1 mole % NBD-POPE. The fluorescence intensity was observed as a function of MARCKS concentration in 100 μM vesicles containing equimolar amounts of SM and Cho, and 20, 40, 60, and 80 mole % POPC (Fig. 12).

Energy transfer was estimated by dividing the NBD emission peak (528 nm) by the MB emission peak (459 nm). No energy transfer increase upon MARCKS addition was seen in any of the POPC vesicles; a decrease was seen in 20% POPC vesicles (Fig. 13). This is interpreted to mean that MARCKS does not cause an increase in domain formation in POPC vesicles. MARCKS probably does not bind well to these vesicles. This also shows that the energy transfer occurring in POPS vesicles results from MARCKS agglutinating the POPS and the probes with it, but not just the probes. If MARCKS were to cluster the probes, energy transfer would be present in the POPC vesicles. Unlike with POPS-containing vesicles, little or no light scatter was observed when MARCKS was added to POPC vesicles, but only a slight drop in fluorescence with the addition of MARCKS. MARCKS probably does not bind to POPC well enough to cause the vesicles to agglutinate or change morphology, which is probably the reason for scattered light in experiments using SM/Cho/POPS vesicles.

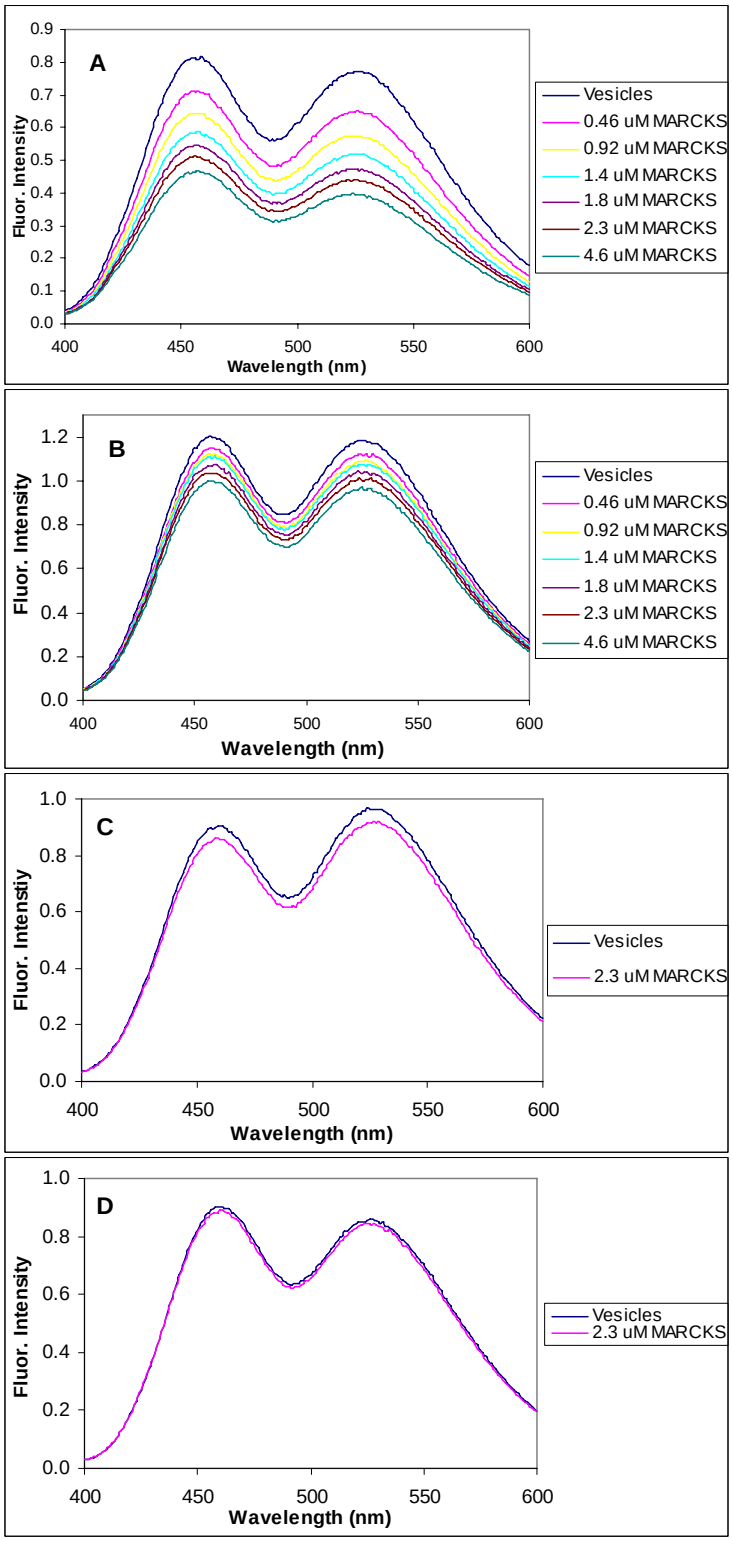

FIGURE 12. Comparison of the experimental fluorescence intensity as a function of MARCKS peptide concentration for various mole percent of the 100 μM SM:Cho:POPC vesicles: **(A)** 40:40:18, **(B)** 30:30:38, **(C)** 20:20:58, **(D)** 10:10:78, where all vesicles contain 1%MB-POPE and 1%NBD-POPE.

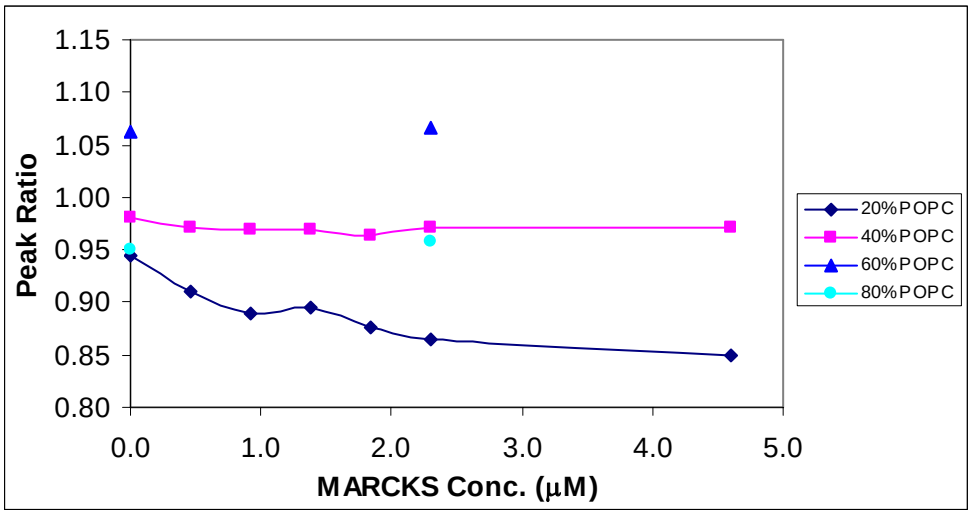

FIGURE 13. Energy transfer as a function of MARCKS concentration in 100 µM vesicles containing equal mole ratios of SM/Cho and 20% POPC, 40% POPC, 60% POPC, or 80% POPC.

Timescales for Domain Formation and Dissipation in SM:Cho:POPS

The timescales of domain formation and dissipation were investigated in SM:Cho:POPS vesicles using stopped-flow fluorescence spectroscopy. Using the information obtained from the steady state fluorescence, the vesicles containing 40 mole % POPS were of the greatest interest since they display the largest increase in energy transfer upon MARCKS addition (Fig. 6).

Domain Formation in SM:Cho:POPS (30:30:40)

Because the addition of MARCKS to vesicles caused a significant increase in light scatter, the fluorescence intensity would appear to decrease with increasing concentration of MARCKS. Thus, MARCKS needed to be present initially at a concentration such that light scatter would have reached a plateau, but not induce the maximum amount of energy transfer. More MARCKS could then be added to observe the increase in domain formation. In Fig. 6 it can be seen that the scattering increased until MARCKS concentration reached 1 μM, where the amount of scattering leveled off. In Fig. 5 it can be seen that energy transfer is still increasing at 1 μM MARCKS, and does not level off until 2.5 μM. The experiments were thus designed taking these considerations into account.

The 200 μM SM:Cho:POPS (30:30:38) 1% MB-POPE, 1% NBD-POPE vesicles were first mixed with buffer to obtain the baseline for energy transfer with 1 μM MARCKS present (concentration after mixing). When the vesicles were mixed with the contents of the other syringe, the final vesicle concentration was 100 μM. A MARCKS concentration of 2.5 μM provided the maximum amount of energy transfer in steady state, therefore the MARCKS concentration used to observe domain formation in stopped flow experiments was 2.5 μM (concentration after mixing). This final MARCKS concentration of 2.5 μM in 100 μM vesicles

was obtained by mixing 4.0 μM MARCKS with the contents in the other syringe (200 μM vesicles and 1.0 μM MARCKS).

Fig. 14 shows the result of an experiment where the vesicles were first mixed with buffer (green), or with MARCKS added to obtain a final concentration of 2.5 μM (blue).
The vesicles were excited at 367 nm (MB excitation) and the emission was observed with time at 535 nm (NBD emission). As seen in Fig. 14, the fluorescence intensity of emission in the vesicles containing 2.5 μM MARCKS was greater than the 1 μM MARCKS baseline. This is the result of increased domain formation after the amount of light scattering had leveled off. In the initial part of the curve corresponding to 2.5 μM MARCKS, there is an initial increase followed by a slower decrease. The initial increase in energy transfer occurred in about 1 s. Because a slow process follows this jump, the domains could have overshot in size. This slower process could be domains relaxing to their equilibrium size, or the vesicle morphology could be changing. (A change in vesicle morphology could cause the light scatter seen with the MARCKS additions.)

Domain Dissipation in SM:Cho:POPS 30:30:40

The timescales for domain dissipation were hypothesized to be much slower than formation, thus dissipation experiments were performed. Using SM:Cho:POPS (30:30:38) vesicles, dissipation could be observed by measuring the emission from vesicles pre-incubated with MARCKS when mixed with vesicles that functioned as acceptors for MARCKS peptide. The pre-incubated vesicles contained 200 μM SM:Cho:POPS (30:30:38), 1% MB-POPE and 1%

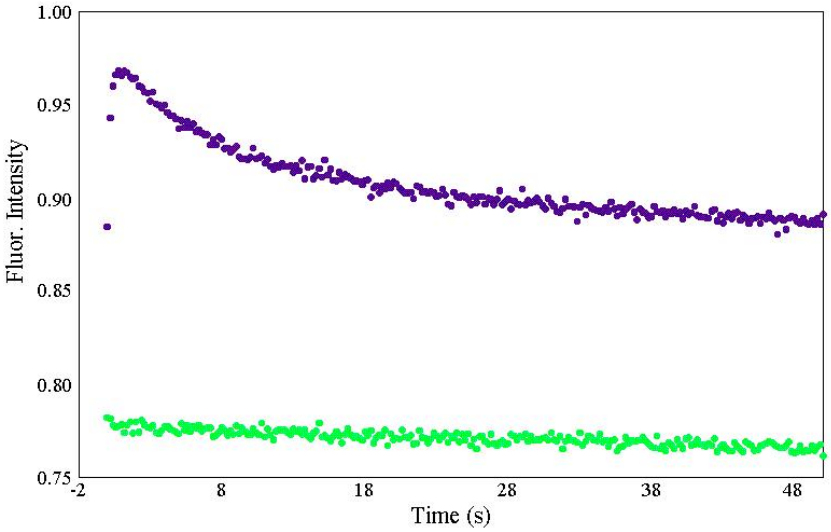

FIGURE 14. Domain formation in 100μM SM:Cho:POPS (30:30:38), 1%MB-POPE and 1% NBD-POPE. The green line is the baseline where vesicles (100 μM) containing 1 μM MARCKS (concentrations after mixing) were mixed with buffer. The blue line is domain formation with a total, final concentration of 2.5 μM MARCKS. The excitation and emission wavelengths were 367 nm and 535 nm, respectively.

NBD-POPE. The MARCKS concentration present in these vesicles was 2.5 μM (concentration after mixing). This allowed domain formation and the corresponding energy transfer to be present before the disruption of the domains occurred. The acceptor vesicles contained 2 mM SM:Cho:POPS (30:30:40), a ten-fold excess of the pre-incubated vesicles, and no probes. Therefore, when the two were mixed in the stopped-flow, the acceptor vesicles bind MARCKS, and the energy transfer decreased as MARCKS left the pre-incubated vesicles and the domains dissipated. The fluorescence intensity was measured at 535 nm (NBD emission) for one hour, with time resolutions of 3, 4, and 10 s.

A baseline was obtained for the 10 s resolution by mixing the 200 μM SM:Cho:POPS (30:30:38), 1% MB-POPE and 1% NBD-POPE having no MARCKS present with the 2 mM SM:Cho:POPS (30:30:40). This revealed that a slower process, probably bleaching, was occurring. The last 2500 s of the dissipation curve provided a good reference for that process. The last 2500 s of each dissipation curve were fit with a straight-line equation, and this equation was subtracted from the curve in order to subtract the slower process that was occurring. The plots were then fitted with a single exponential equation,

$$y = A\,e^{\left(\frac{-t}{\tau}\right)} + B$$

where A is the amplitude of the curve, t is time, τ is the apparent relaxation time, and B is the y-intercept. These plots can be seen in Fig. 15 A, B, and C. The timescales for the plots are given by τ: approximately 620 s, 597 s, and 1330 s for the resolution of 3 s, 4 s, and 10 s, respectively. The average is 900 ± 400 s.

These timescales include not only the time it takes for domains to dissipate, but also the time it takes for MARCKS to dissociate from the membrane. In order to determine the time for the dissipation event only, the time required for MARCKS dissociation needed to be determined.

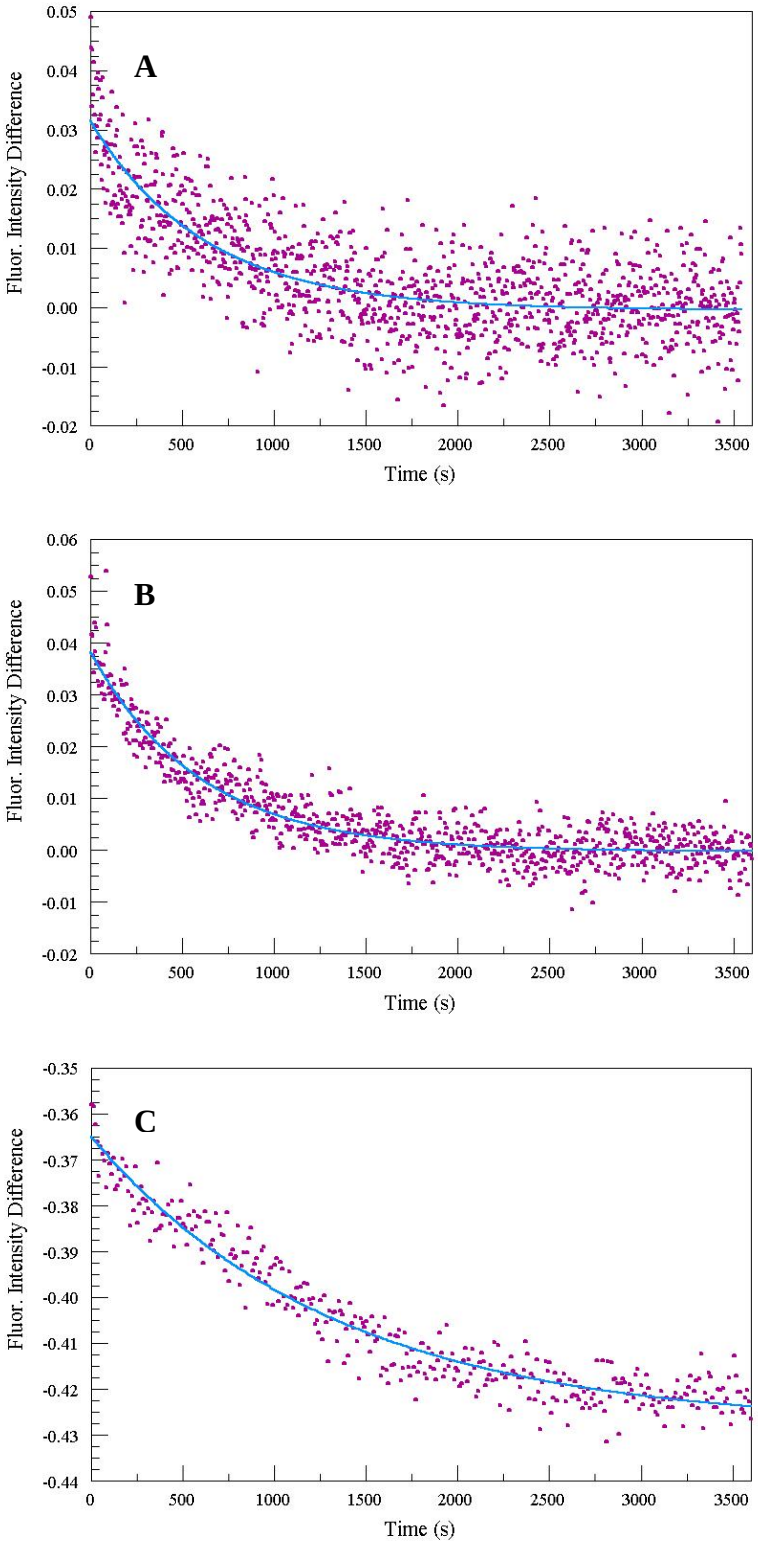

FIGURE 15. Domain dissipation in 100μM SM:Cho:POPS (30:30:38), 1% MB-POPE and 1% NBD-POPE for one hour with resolution of 3 s **(A)**, 4 s **(B)**, and 10 s **(C)** (concentration after mixing).

This was achieved using MARCKS labeled with NBD at its N-terminus and vesicles containing MB-POPE. When the NBD-MARCKS is bound to the membrane, energy transfer will occur between the MB in domains in the vesicles and the NBD on MARCKS. When MARCKS is removed with acceptor vesicles, the MARCKS binds to the acceptor vesicles and is no longer in close proximity to the MB in the donor vesicles. This causes energy transfer to decrease, which could be seen as a decrease in fluorescence intensity at the NBD emission wavelength (535 nm). The timescale for this process represents the timescale for MARCKS to dissociate from the membrane.

The timescale for MARCKS removal in SM:Cho:POPS 30:30:40 vesicles was determined using the same conditions as the domain dissipation experiments. The pre-incubated vesicles (200 μM) contained SM:Cho:POPS (30:30:39) and 1% MB-POPE and 2.5 μM NBD-MARCKS. The acceptor vesicles (2 mM) contained (SM:Cho:POPS (30:30:40). The two were mixed and the emission of NBD was measured for approximately one half hour. The plot for the off-rate of MARCKS was fitted with a single exponential equation, and the timescale was determined (Fig. 16).

A decrease in fluorescence intensity represents the decrease in energy transfer that occurs when MARCKS is removed from the vesicles. The value of τ was determined to be 275 s for the removal of MARCKS, which is shorter than observed in the domain dissipation experiments. This means that MARCKS dissociating from the membrane was not the only timescale that was measured in the first experiments; there was a second, slower process occurring. This slower process is interpreted to be the dissipation of lipid domains.

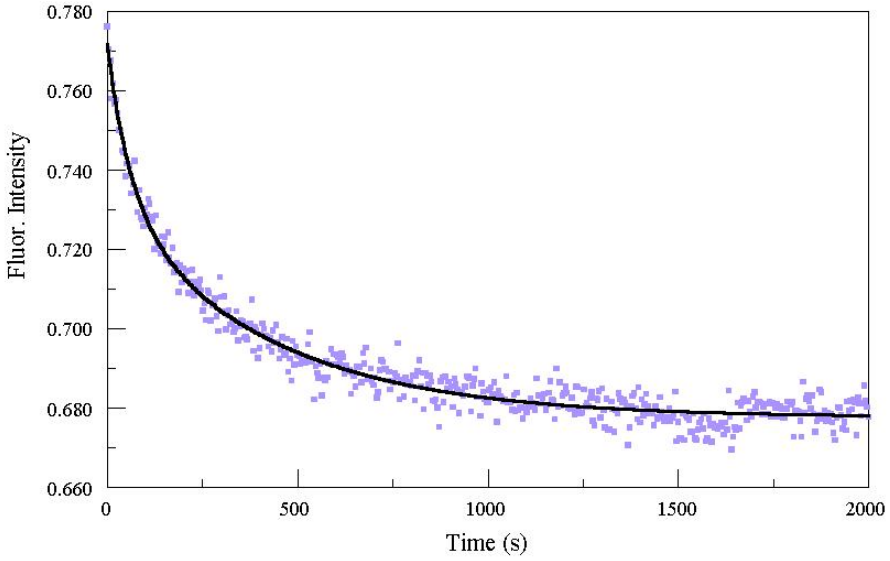

FIGURE 16. Timescale of NBD-MARCKS removal from membrane in 100μM SM:Cho:POPS (30:30:39) and 1% MB-POPE mixed with 1 mM SM:Cho:POPS (30:30:40) (concentrations after mixing).

Domain Dissipation in SM:Cho:POPS 45:45:10

Domain dissipation was also measured in vesicles containing sphingomyelin, cholesterol and 10% POPS to determine the timescales in vesicles containing a small concentration of POPS. Using vesicles containing SM:Cho:POPS (45:45:8), 1% NBD-POPE and 1% MB-POPE, dissipation could be observed by measuring the emission of vesicles pre-incubated with MARCKS when mixed with 10-fold excess vesicles that contain no probes and function as acceptors for the MARCKS. The dissipation was observed as a function of time when the two were mixed for approximately ten minutes. The dissipation experiment was performed using resolutions of 1 and 4 s. The average of several runs was plotted for each, and a single exponential curve:

$$y = A\left(1 - e^{\left(\frac{-t}{\tau}\right)}\right) + B,$$

was fit to the data (Fig. 17) and τ was determined to be 160 s in both experiments.

Unlike the 40 mole % POPS-containing vesicles, the fluorescence intensity increases when the domains relax to their equilibrium size. In the 10 mole % POPS- containing vesicles, there is much less POPS present, which would mean that there were fewer or smaller domains present. When the MARCKS is bound to the membrane, it may separate the POPS and probes, competing for the few negative charges present in the vesicles. When the MARCKS is removed, it may be that, when the domains relax to their equilibrium size, they form larger domains than when the MARCKS is present. Thus, the increase in fluorescence probably arises from having larger domains in the absence of MARCKS in this case.

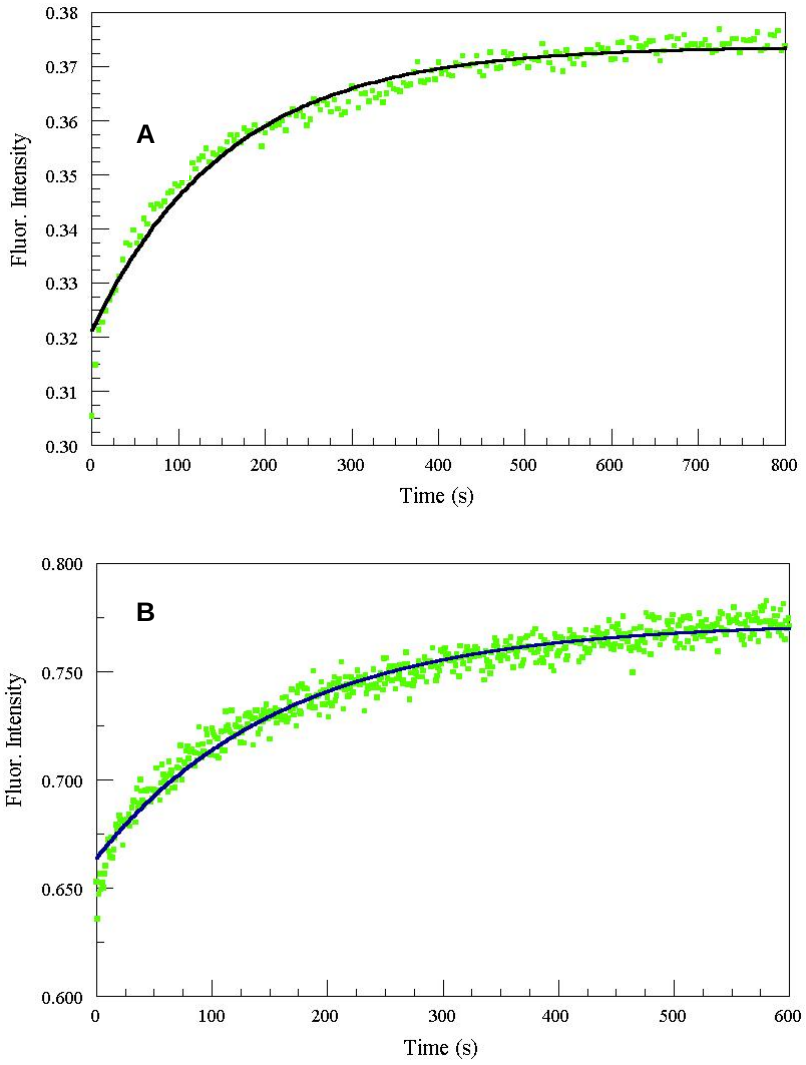

FIGURE 17. Domain dissipation in 100μM SM:Cho:POPS (45:45:8), 1% MB-POPE and 1% NBD-POPE for one hour with resolution of 4 s **(A)**, 1 s **(B)** (concentration after mixing).

Again, the timescale for the off-rate of MARCKS in 10 mole % POPS was determined using NBD-MARCKS. Vesicles with 200μM lipid of SM:Cho:POPS (45:45:8) containing 1% MB-POPE were pre-incubated with 2.5μM NBD-MARCKS. The acceptor vesicles contained 2 mM SM:Cho:POPS (45:45:8), thus a ten-fold excess. The emission of NBD with time was measured for about 10 minutes and a two exponential decay was fit to the data (Fig. 18). The equation for the curve is

$$y = A\left((1 - A_2)\, e^{\left(\frac{-t}{\tau_1}\right)} + A_2\, e^{\left(\frac{-t}{\tau_2}\right)} \right) + B$$

where A is a global amplitude factor, $(1\text{-}A_2)$ is the amplitude of the first process, A_2 is amplitude of the second process, τ_1 is the inverse of the apparent rate constant for the fast process, τ_2 is the inverse of the apparent rate constant for the slow process, t is time, and B is the y-intercept.

The first τ was calculated to be about 1 s, which was interpreted to be the timescale for MARCKS dissociation from the membrane. This can be seen in Fig. 18B. The second process, τ_2, was calculated to be 100 s, and this was interpreted as a slower relaxation process that occurs after the MARCKS comes off the membrane. This probably corresponds to the domain dissipation, which was measured to occur in 160 s, above.

Dynamics of Domains in Other Lipid Mixtures

Vesicles composed of di-14:1PC and POPS were chosen in order to study the dynamics of domains in vesicles containing different types of lipids. Di-14:1PC has shorter chains than POPS which makes their interactions with each other less favorable than between di-14:1PC with itself and POPS with itself. Thus, POPS domains could be easily formed with the

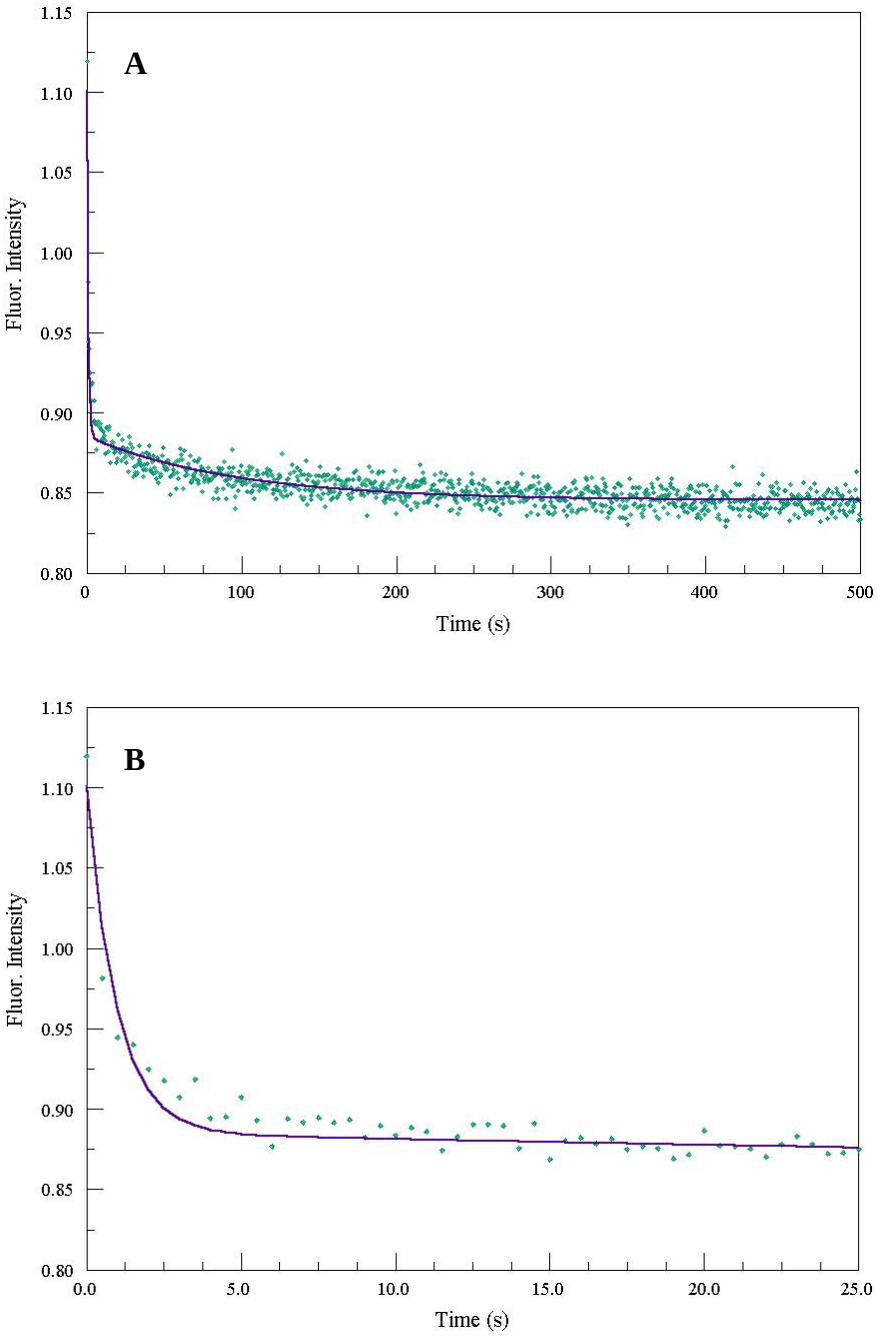

FIGURE 18. Removal of NBD-MARCKS from membrane in 100μM SM:Cho:POPS (45:45:8), 1% MB-POPE and 1% NBD-POPE for 500 s **(A)**, and the same plot for the first 25 s **(B)** (concentration after mixing).

introduction of MARCKS peptide. The domain formation was monitored using the energy transfer pair MB-POPE and NBD-POPE, as before.

Steady State Fluorescence

Vesicles containing di-14:1PC:POPS (80:18), 1%MB-POPE and 1%NBD-POPE were observed with fluorescence in steady state. The probe concentrations that resulted in the highest sensitivity to peptide addition were determined to be the same as the concentrations used in the SM/Cho vesicles. MB-POPE was excited at 367 nm, and the emission was scanned from 400 nm to 600 nm. The fluorescence intensity was observed as a function of MARCKS concentration in 100μM vesicles containing 20 mole % POPS. As seen in Fig. 19, there is an increase in energy transfer with the addition of 2.3 μM MARCKS, which was interpreted as an increase in domain formation.

Domain Dissipation in Di-14:1PC:POPS

Domain dissipation was observed by stopped-flow fluorescence to determine the timescale for this process. Dissipation was observed by measuring the emission from vesicles pre-incubated with MARCKS, which were mixed with vesicles containing no probes, in ten-fold excess, which function as acceptors for MARCKS. The pre-incubated vesicles contained 200 μM di-14:1PC:POPS (80:18), 1% MB-POPE and 1% NBD-POPE. The MARCKS concentration present in the pre-incubated vesicles was 2.5 μM.

This allowed domain formation and the corresponding energy transfer to be present before MARCKS was removed. The MB-POPE was excited at 367 nm, and the emission was observed at 535 nm for about 50 s (Fig. 20). The curves were fit with a single exponential and

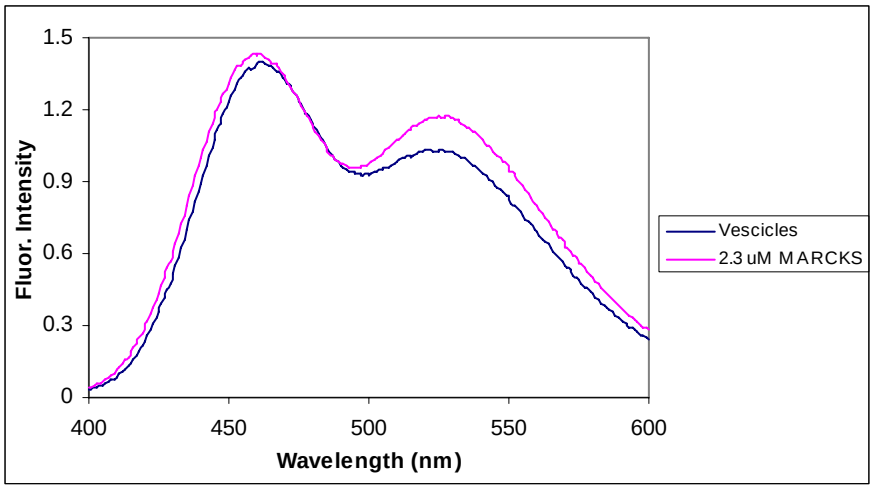

FIGURE 19. Fluorescence intensity with the addition of MARCKS peptide in 100 μM vesicles (concentration after mixing) containing di-14:1PC:POPS (80:18), 1% MB-POPE and 1% NBD-POPE.

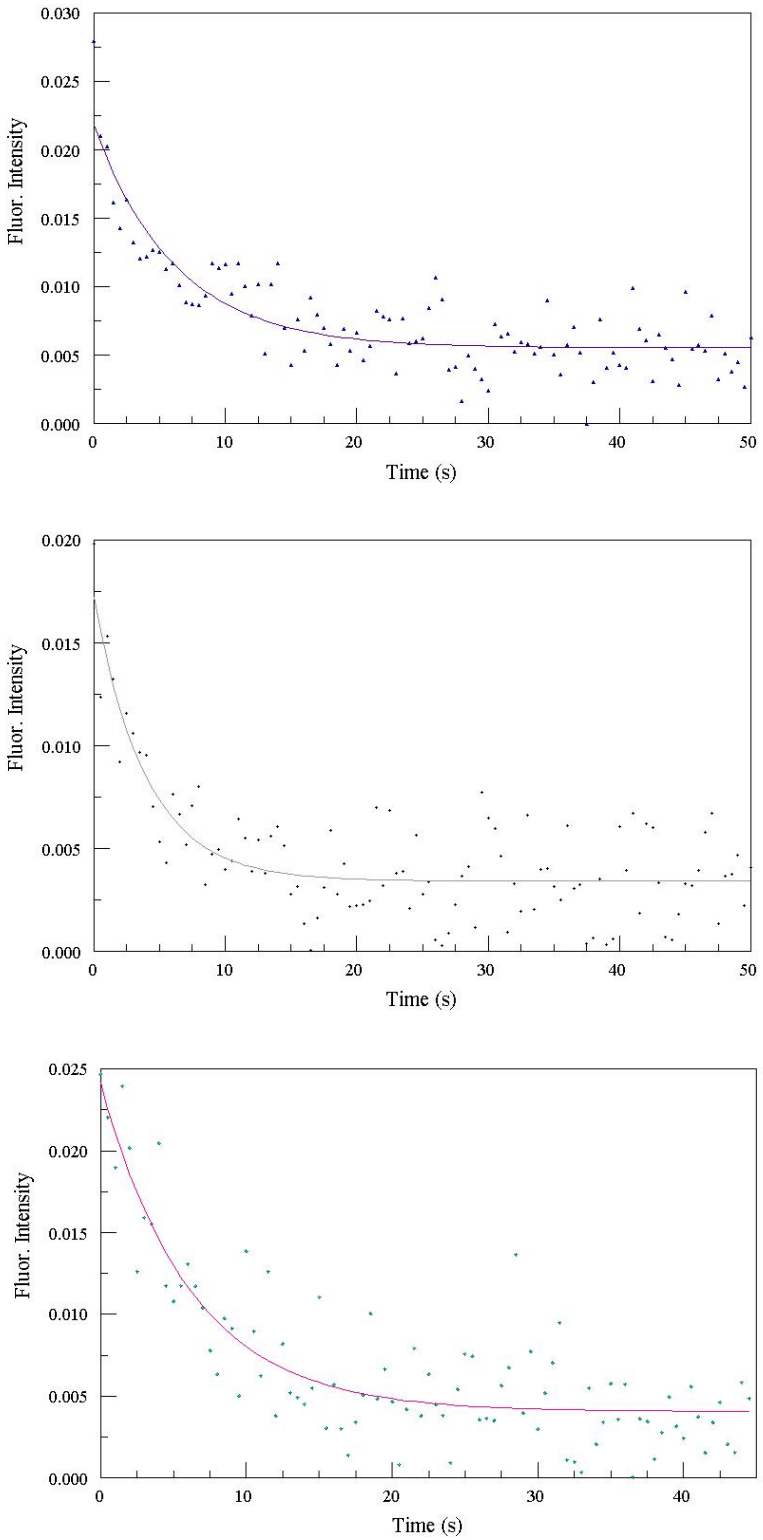

FIGURE 20. Domain dissipation with time in 100 μM di-14:1PC:POPS (80:18), 1% MB-POPE and 1% NBD-POPE with 0.5 mM acceptor vesicles **(A)**, and 1 mM acceptor vesicles **(B)** and **(C)** (concentrations after mixing).

the values of τ were as follows: 4 s for Fig. 20A, and 6 s for both 20B and 20C. The average value of τ was 5 ± 1 s.

Summary of Dynamics

The timescales for MARCKS desorption and domain dissipation for SM:Cho:POPS 30:30:40, SM:Cho:POPS 45:45:10, and di-14:1PC:POPS can be seen in Table 1. The table summarizes the rates measured in this work, and also includes the calculated rate for MARCKS desorption for di-14:1PC:POPS.

Lipid Mixture	MARCKS Desorption (s)	Domain Dissipation (s)
SM:Cho:POPS(30:30:40)	275	900 ± 400
SM:Cho:POPS (45:45:10)	1	160
di-14:1PC:POPS (80:20)	< 1*	5 ± 1

*calculated τ from k_{off} which is described in the conclusion

TABLE 1. Summary of timescales for MARCKS desorption and domain dissipation

CONCLUSION

Domain formation and dissipation were observed using vesicles of various mole percents of sphingomyelin, cholesterol, and POPS, with several different compositions, containing the energy transfer pair MB-POPE and NBD-POPE. The domains were induced using the MARCKS peptide. Because MARCKS contains 13 positive charges, it agglutinates negatively charged lipids. POPS, MB-POPE, and NBD-POPE are anionic overall, thus MARCKS agglutinated them in domains.

In steady state, light scatter increased upon MARCKS addition to the vesicles, which was probably from vesicle aggregation or a change in vesicle morphology caused by MARCKS aggregation. Vesicle aggregation did not cause a significant amount of energy transfer to occur between vesicles. The efficiency of energy transfer was measured and determined to be independent of light scatter.

The timescales for domain formation and dissipation were observed in vesicles of sphingomyelin, cholesterol, and POPS with the energy transfer pair MB-POPE and NBD-POPE. The kinetics were measured by stopped-flow fluorescence. Domain formation in SM:Cho:POPS (30:30:40) 1%MB-POPE, 1%NBD-POPE was less than 1 s, which was then followed by a slower relaxation process. Domain dissipation in 40 mole % POPS was approximately 900 s and domain dissipation in 10 mole % POPS was approximately 160 s.

Previous studies have investigated the relaxation dynamics of vesicles in nonequilibrium phase separation processes. Van Osdol et al (*24*) found the relaxation dynamics of the gel-to-liquid crystalline transition to be extremely rapid. This was observed in five phosphatidylcholine bilayer dispersions of varying chain length, from

di-C14:0PC to di-C18:0PC. The relaxation times had a pronounced maximum at a temperature near T_m for MLVs, which varied from approximately 50 ms to 4 s; LUVs had a relaxation time of about 80 ms.

Jørgensen et al (*25*) examined the nonequilibrium ordering dynamics of lipid domains in the gel-fluid coexistence region of an equimolar di-C16:0PC:di-C22:0PC lipid mixture. The vesicles were quenched, which means they were subjected to a sudden temperature drop from the fluid to the gel-fluid coexistence region. The reorganization of the lipids was observed as they relaxed from nonequilibrium to equilibrium domains. The relaxation times observed occurred in a timescale of approximately 2×10^3 s. De Almeida et al (*26*) also investigated the relaxation times after quenching in a two-component lipid bilayer with acyl chain mismatch in a di-C12:0PC/di-C18:0PC lipid mixture. The times ranged from approximately 2×10^3 s to approximately 12×10^3 s.

These timescales are much slower than the ones obtained here in the SM:Cho:POPS experiments. This is expected because the timescales in the PC lipid mixtures were obtained in the gel-fluid region, whereas the SM:Cho:POPS vesicles were in the liquid phase having both liquid-ordered (l_o) and liquid-disordered (l_d) phase.

The kinetics of MARCKS association and dissociation have recently been studied (*1*, *27*). Arbuzova et al (*27*) determined the dissociation rate constant, k_{off}, by measuring the rate at which MARCKS peptide moves from donor to acceptor vesicles using resonance energy transfer between a fluorophore on the peptide and NBD on POPC:POPS vesicles (*27*). k_{off} can be approximated as the inverse of τ because the acceptor vesicles were in excess (*27*). The dissociation rate constants measured using this method were 6 s^{-1} for 10% POPS-containing vesicles and 1.5 s^{-1} for 20% POPS-containing vesicles. The value for τ for 20% POPS was

calculated to be < 1 s, which is the inverse of k_{off}, and is shown in Table 1 for 14:1PC:POPS (80:20). This calculated value was reported in the table because the off-rate of MARCKS was not determined experimentally for di-14:1PC:POPS (80:20). The k_{off} calculated from τ in SM:Cho:POPS (45:45:8) was approximately 1 s^{-1}, which is close to the 6 s^{-1} reported in POPC:POPS vesicles by Arbuzova et al (*27*).

The association rate constant for MARCKS, k_{on}, was determined to be diffusion limited and was reported to be 10^{11} $M^{-1}s^{-1}$ per vesicle (*27*), thus k_{on} is 10^6 $M^{-1}s^{-1}$ per lipid. Rusu et al (*1*) reported the binding of MARCKS to POPC:POPS vesicles, varying the ratio of POPC and POPS. The peptide bound strongly to vesicles with a high fraction of POPS and weakly to those with a low fraction of POPS. The binding constant increases exponentially with the mole fraction of POPS in the vesicles. The binding constants were estimated to be 10^5 M^{-1} per lipid for 10% POPS-containing vesicles and 10^7 M^{-1} per lipid for 20% POPS-containing vesicles.

Using the association rate of MARCKS and the value of τ from SM:Cho:POPS (30:30:40) MARCKS dissipation experiment, the molar partition coefficient, also known as the binding constant, K, for SM:Cho:POPS (30:30:40) was estimated using the equation (*27*):

$$K = \frac{k_{on}}{k_{off}} = \frac{k_{on}}{1/\tau},$$

yielding a value for K of approximately 3×10^9 M^{-1}.

The processes of MARCKS desorption and domain dissipation can be represented using the following model:

$$A \xrightarrow{k_1} B \xrightarrow{k_2} C$$

where A represents a system where MARCKS is bound to the membrane and domains exist, k_1 is the rate of MARCKS dissociation, B represents a system where MARCKS is not bound and the

lipids are in non-equilibrium, k_2 is the rate of domain dissipation, and C is a state where the lipids are in equilibrium.

The off-rate of MARCKS, or k_1 in the model above, had been studied in similar systems. However, the rates of domain dissipation, or k_2 in the model, had not yet been measured. This work represents a first attempt at their determination. These timescales are of great interest and should be investigated further, especially in raft-containing vesicles, because they could provide insight for cellular processes such as signal transduction.

REFERENCES

1. Rusu, L., Gambhir, A., McLaughlin, S., and Rädler, J. (2004) Fluorescence correlation spectroscopy studies of peptide and protein binding to phospholipid vesicles. *Biophys.. J. 87*, 1044-1053.

2. Hinderliter, A., Biltonen, R.L., and Almeida, P.F.F. (2004) Lipid modulation of protein-induced membrane domains as a mechanism for controlling signal transduction. *Biochemistry 43*, 7102-7110.

3. Hinderliter, A., Almeida, P.F.F., Cruz, C.E., and Biltonen, R.L. (2001) Domain formation in a fluid mixed lipid bilayer modulated through binding of the C2 protein motif. *Biochemistry 40*, 4181-4191.

4. McMullen, T.P.W., Lewis, R.N.A.H., and McElhaney, R.N. (2004) Cholesterol-phospholipid interactions, the liquid-ordered phase and lipid rafts in model and biological membranes. *Curr. Opin. Colloid Interface Sci. 8*, 459-468.

5. Edidin, M. (2003) The state of lipid rafts: from model membranes to cells. *Annu. Rev. Biophys. Biomol. Struct. 32*, 257-283.

6. Silvius, J.R. (2002) Role of cholesterol in lipid raft formation: lessons from lipid model systems. *Biochim. Biophys. Acta*, 174-183.

7. Fielding, C.J., and Fielding, P.E. (2003) Relationship between cholesterol trafficking and signaling in rafts and caveolae. *Biochim. Biophys. Acta*, 219-228.

8. Simons, K., and Ikonen, E. (1997) Fuctional rafts in cell membranes. *Nature 387*, 569-572.

9. Jørgensen, K., and Mouritsen, O.G. (1995) Phase separation dynamics and lateral organization of two-component lipid membranes. *Biophys. J. 95*, 942-954.

10. Addadi, L., Geva, M., and Kruth, H.S. (2003) Structural information about organized cholesterol domains from specific antibody recognition. *Biochim. Biophys. Acta*, 208-216.

11. Simons, K., and Vaz, W.L.C. (2004) Model systems, lipid rafts, and cell membranes. *Annu. Rev. Biophys. Biomol. Struct. 32*, 269-295.

12. Ipsen, J.H., Karlstrom, G, Mouritsen, O.G., Wennerstrom, H., and Zuckermann, M.J. (1987) Phase equilibria in the phosphatidylcholine-cholesterol system. *Biochim. Biophys. Acta 905*, 162-172.

13. Ipsen, J.H., Mouritsen, O.G., Zuckermann, M.J. (1989) Theory of thermal anomalies in the specific heat of lipid bilayers containing cholesterol. *Biophys. J. 56*, 661-667.

14. Collado, M.I., Goñi, F.M., Alonso, A., and Marsh, D. (2005) Domain formation in sphingomyelin/cholesterol mixed membranes studied by spin-label electron spin resonance spectroscopy. *Biochemistry 44*, 4911-4918.

15. Arbuzova, A., Murray, D., and McLaughlin, S. (1998) MARCKS, membranes, and calmodulin: kinetics of their interaction. *Biochim. Biophys. Acta 1376*, 369-379.

16. Faircloth, R.H., and Cantor, C.R. (1977) The use of singlet-singlet energy transfer to study macromolecular assemblies. *Methods Enzymol. 48*, 347-379.

17. Kates, M. (1972) Techniques of Lipidology, in *Laboratory Techniques in Biochemistry and Molecular Biology* (Work, T. S., and Work, E., ed.) 1st ed., p.421, North-Holland Publishing Company, Amsterdam.

18. Pokorny, A., Birkbeck, T.H., and Almeida P.F.F. (2002) Mechanism and kinetics of δ-lysin interaction with phospholipid vesicles. *Biochemistry 41*, 11044-11056.

19. Haugland, R.P. (2002) *Handbook of Fluorescent Probes and Research Products* (9th ed.). Eugene, Oregon: Molecular Probes, Inc.

20. Bradford, M.M. (1976) A rapid and sensitive method for the quantitation of microgram quantities of protein utilizing the priniciple of protein-dye binding. *Anal. Biochem. 72*, 248-254.

21. Udenfriend, S., Stein, S., Bohlen, P., Dairman, W., Leimgruber, W., and Weigele, M. (1972) Fluorescamine: a reagent for assay of amino acids, peptides, proteins, and primary amines in the picomole range. *Science 178*, 871-872.

22. Lackowicz, J.R. (1999) Energy Transfer in *Principles of Fluorescence Spectroscopy* 2nd ed., p.381, Kluwer Academic/Plenum Publishers, New York.

23. Skoog, D.A., Holler, F.J., and Nieman, T.A. (1998) *Principles of Instrumental Analysis* (5th ed.). Florida:Harcourt Brace & Company.

24. van Osdol, W.W., Johnson, M.L., Qiang Ye, and Biltonen, R.L. (1991) Relaxation dynamics of the gel to liquid-crystalline transition of phosphatidylcholine bilayers: effects of chainlength and vesicle size. *Biophys. J. 59*, 775-785.

25. Jørgensen, K., Klinger, A., and Biltonen, R.L. (2000) Nonequilibrium lipid domain growth in the gel-fluid two-phase region of a $DC_{16}PC$-$DC_{22}PC$ lipid mixture investigated by Monte Carlo computer simulation, FT-IR, and fluoresescence spectroscopy. *Biophys.J. 104*, 11763-11773.

26. de Almeida, R.F.M., Loura, L.M.S., Fedorov, A., and Prieto, M. (2002) Nonequilibrium phenomena in the phase separation of a two-component lipid bilayer. *Biophys. J. 82*, 823-834.

27. Arbuzova, A., Wang, J., Murray, D., Jacob, J., Cafiso, D.S., and McLaughlin, S. (1997) Kinetics of interaction of the myristoylated alanine-rich C kinase substrate, membranes, and calmodulin. *J. Biol. Chem. 272(43)*, 27167-27177.